



Experimental study of residual stresses in thick steel plates

R. Thiébaud¹, J.-P. Lebet²

Abstract

Residual stresses must be taken into account when evaluating the stability of a steel bridge girder. Residual stresses are unavoidable, as manufacturing processes for steel plates introduce thermal residual stresses in the material. For welded built-up sections, such as those commonly used in large steel plate girders, these thermal residual stresses are due to 1) cooling after rolling, 2) flame cutting of the flanges, and 3) welding between the web and the flange. Residual stresses can influence the lateral torsional buckling resistance of structural steel members and need to be considered in design.

This paper experimentally investigates residual stresses due to flame cutting using the sectioning method. In this study, residual stresses are measured after flame cutting and welding 60 mm thick steel (S355N) flanges, a typical size used in the fabrication of bridge girders. Results from flame cutting confirm the findings of previous studies which reveal that residual stress distributions have a high tensile component at the flame cut edge. Procedures and testing of welding residual stresses are also presented.

Residual stress measurements from this study could be used to develop a longitudinal and through-thickness residual stress model for thick flame-cut plates and welded plates used in bridge I-girder construction. Such a model could serve as an initial state in non-linear finite element analyses to predict the residual stress influence on the LTB of steel bridge girders.

1. Introduction

Built-up steel plate girders used in bridges are often constructed using rolled steel plates welded together. Due to manufacturing and assembly of the steel plates, residual stresses are often introduced into the girder section. Combined with high slenderness ratios (height/width ratio), geometric imperfections, and dynamic traffic loads, residual stresses can create stability issues, namely lateral torsional buckling (LTB) (see Fig. 1).

The complex phenomenon of LTB is well established in design standards; however the current design standards are based on experimental and theoretical studies on rolled I-sections and built-

¹ PhD student, ÉCOLE POLYTECHNIQUE FÉDÉRALE DE LAUSANNE (EPFL), School of Architecture, Civil and Environmental Engineering (ENAC), Steel Structures Laboratory (ICOM), raphael.thiebaud@epfl.ch.

² Professor, ÉCOLE POLYTECHNIQUE FÉDÉRALE DE LAUSANNE (EPFL), School of Architecture, Civil and Environmental Engineering (ENAC), Steel Structures Laboratory (ICOM), jean-paul.lebet@epfl.ch.

up sections having common building-section geometries. Steel plate-girders used in bridges are often much larger and have different geometric properties than typical building sections. The LTB resistance models for plate girders are adapted from data on typical rolled sections with reduction factors (Davaine and Lebet, 2007).

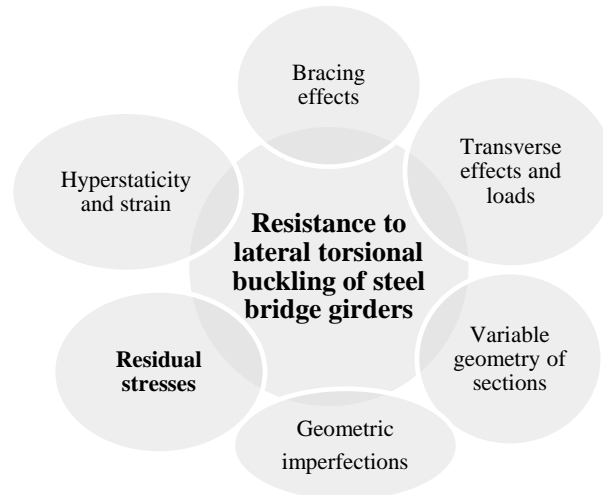


Figure 1: Mains parameters which influence the LTB resistance of steel bridge girders.

Several residual stress models already exist in the literature. Some are based on thin plates (ECCS, 1984, Johansson et al., 2007), and others are based on thicker plates comparable with the plates used in this study (Alpsten and Tall, 1969, Brozzetti, 1969, Bjorhovde et al., 1971, ECCS, 1976). Residual stresses form a self-equilibrating system, where resultant forces and moments are zero. In general, as explained by (Lu, 1996) there are three principal kinds of residual stresses. The first, named macroscopic residual stress, concern at least several grains of the material. The second, termed structural micro-stress, applies to the distance of one grain or a part of a grain. The third corresponds to several atomic distances within the grain and is equilibrated over a small part of the grain.

This paper describes an experimental study investigating longitudinal macroscopic residual stresses in thick steel plates due to flame cutting and welding. First, the appropriate methods for residual stress measurements are briefly presented. Following, the experimental work is discussed, including the materials used, fabrication and preparation of the test specimens, the flame cutting and welding procedure, and temperature measurements. Lastly, results for flame-cutting residual stresses are presented and conclusions are summarized.

Further study to be completed later will create a residual stress model from the experimental data accounting for welding and the flame-cutting of thick steel plates, and incorporating the model into finite element analyses to study the LTB resistance of steel plate girders.

2. Methods and measurements

2.1 Residual stress measurement techniques

This section presents an overview of common methods used to measure residual stresses. In general a distinction must be made between destructive and non-destructive techniques (Lu, 1996).

The destructive methods break the state of equilibrium of the residual stresses by a mechanical process. Residual stresses determined by mechanical process are partially or completely released when material is removed. Material relaxation creates a displacement which can be measured allowing the stresses to be calculated. Some well-known destructive techniques include sectioning, hole drilling and layer removal, and some others in development include the contour and deep hole methods. Furthermore, it is important to note that the sectioning method provides single stress measurements, the hole drilling method provides depth profiles, and the contour method provides area maps of residual stress. As shown in Fig. 2 these methods are represented in function of the depth penetration and the spatial resolution which give the application domain.

The non-destructive methods use the relationship between the physical or crystallographic parameters and the residual stress. The X-ray and neutron diffraction methods are based on the measurements of lattice strains of specific atomic planes. The first technique measures residual stress on the surface, but it is available until 1 mm penetration by combination with the destructive layer removal method (Fig. 2). The neutron diffraction method measures the residual strain within a volume of sample; therefore it is valid for larger penetrations up to 50 mm. Ultrasonic techniques rely on variations of velocity of ultrasonic waves, which can be related to the residual stress state. Magnetic measuring methods are based on the interaction between magnetization and elastic strain in ferromagnetic materials. The application domain of this experimental study is located in a spatial resolution of around 10 mm and a penetration of several centimeters. Accordingly to Fig. 2 the sectioning and the deep hole drilling methods are available to evaluate residual stresses in thick plates. However, the equipment available within our laboratory is suitable to the sectioning method which is further discussed in the following section.

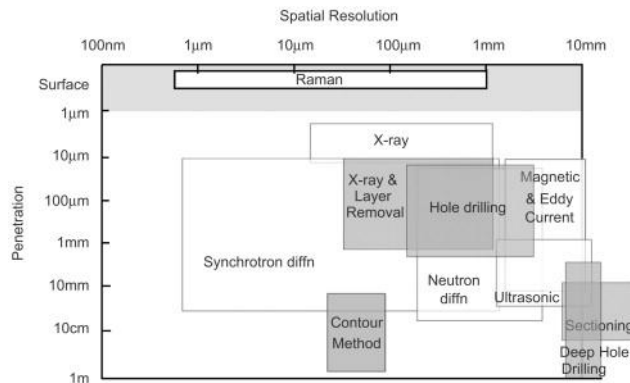


Figure 2: Schematic indicative of the approximate current capabilities of the various techniques to measure residual stresses. The destructive techniques are shaded grey. (Withers et al., 2008)

2.2 The sectioning method

In order to release the internal stresses, the sectioning method proposes to isolate a specimen and cut it into many strips and slices (Fig. 3). This technique, commonly use in steel construction, is suitable for elements in which the longitudinal stresses are dominant. Several experiences performed in the past prove that the sectioning method is adapted to this kind of measurements, sufficiently accurate and economical (Tebedge et al., 1973, Aschendorff et al., 1983, Grimault and Rondal, Lugeon and Sriramulu, 1978). One important advantage is in the method implementation, which is relatively simple and feasible with the equipment of our laboratory.

As illustrated by the Fig. 3, the sectioning method counts three main steps. First, a basis of measurement must be implemented on the initial steel plate. This basis consists to mark a series of parallel points all around the steel plate. These points produce distances which are measured so as to create the initial values. Secondly transverse pieces, which represent the specimens, are isolated by sawing the initial steel plate, Fig. 3a. Then, the specimens are cut in strips to perform a complete sectioning of the specimen, Fig. 3b. Next, the basis of points is measured once again to obtain the change of length of each strip. Thus the distribution of longitudinal strains over a cross section is determined and the stresses can be calculated by applying Hooke's law. The third and last step concerns the cutting of each strip in slices, Fig. 3c. The slicing provides the residual-stress distribution through the thickness by measuring the change of strain of each slice after cutting. A base measurement must be implemented on each side of each strip.

The determination of the residual stress with the sectioning method includes some assumptions. Firstly, the analysis is simplified by not taking into account the effect of the transverse stresses. In fact it is known (Tebedge et al., 1973) that transverse stresses affect the results; with lower transverse stress leading to more accurate measurements. A second assumption is based on the process to cut the pieces in strips and slices. During this process, the material is heated by the saw, in other words residual stresses are created by the sawing. These additional stresses depend on many factors such as the saw cut spacing, the thickness of the plate and the speed of sawing. Measurements considering this effect were performed for one specific case (Alpsten and Tall, 1969) at the saw cut edge and stresses of the order of 3-10 MPa were observed. Furthermore, temperatures measurements were carried out during our experiments. The results show that the temperature vary on a scale of 20 to 30°C at maximum on the steel cut surface between before and after cutting. These values can be lowered by an efficient system of liquid cooling during the sawing. Again, in comparison with the temperature measured during the flame-cutting and the welding, which reach several hundreds to thousands of degrees Celsius, the saw heating values are low.

Finally, if care is taken by a clean preparation of the specimens, a methodic and rigorous procedure of measurement, the sectioning method provides suitable and accurate results.

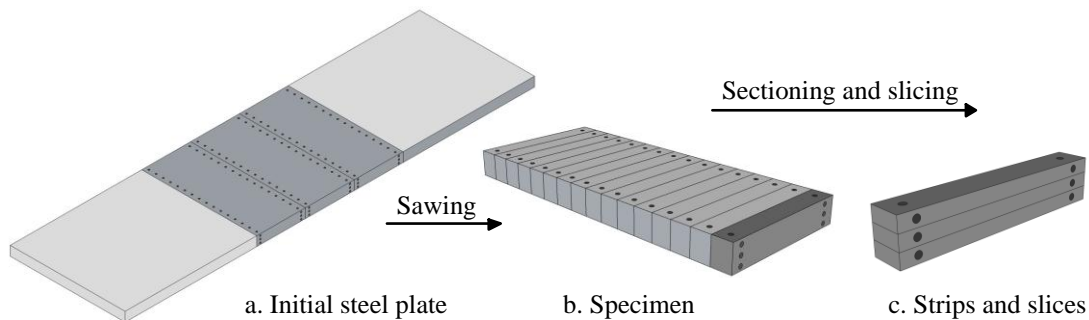


Figure 3: Main steps in the sectioning method.

3. Experimental work

3.1 Materials

The choice of the materials is based on those commonly used in bridge construction and available from the firm (Table 1). Thus, the base plate PL60 (Fig. 4), which corresponds to the flanges of the built-up sections, is a normalized rolled weldable fine grain structural steel S355N. The web corresponds to a non-alloy structural steel S355J2. Designation of the plates follows the Eurocodes (CEN, 2004b, CEN, 2004c, CEN, 2004d, CEN, 2004e, CEN, 2004a, CEN, 2005).

Table 1: Materials and dimensions

Part	Grade	Quality	Length (mm)	Width (mm)	Thickness (mm)
Base plate	S355	N	2600	2100	60
Web	S355	J2	2600	180	20

Regarding the dimensions the two following criterions were taken into account:

- the sizes of the plates have to represent those used to manufacture built-up sections of bridge girders
- the final size of the welded section allowed the application of the sectioning method for the residual stress study

3.2 Fabrication of the specimens and temperature measurements

The manufacturing of steel bridge girders follows two main processes. First the steel plates (flanges, webs, etc...) which constitute the girders are flame-cut on plates ordered from the steel factories. Secondly, these pieces are assembled together by different methods of welding. Both steps introduce stresses which modify significantly the prior residual stresses due after rolling. In the following, the two processes used to fabricate the specimen and the temperature measurements are briefly presented.

3.2.1 Flame-cutting

Flame-cutting is the principal process for cutting steel plates and form a part of thermal cutting. This technology uses gases, propane and oxygen to produce a controlled flame. The principle is based on a chemical reaction of oxygen with the base metal at elevated temperatures. More precisely, the material is heated locally via a flame obtained from the combustion of a specific fuel gas mixed with oxygen. Then, the metal is burned by a jet of pure oxygen creating a continuous chemical reaction between the oxygen and the metal. Finally, the iron oxide formed is blown away by the jet of oxygen which creates a cut and a heat affected zone (HAZ). (Brune, 2011).

In this study, the base plate was flame-cut into three pieces named “flanges” (Fig. 4) with a numerical control machine. The direction of cutting corresponds to the rolling direction and was performed with a speed of 250 mm/min. This velocity depends mainly on the type of material and the material thickness. The sequencing consists of three cuts performed successively by the same torch. The widths of the flame-cut flanges are 730 mm for T1 and T2b and 615 mm for T2a. The plate T2b is devoted to the welding and flame-cutting study whereas T1 and T2a are dedicated to the flame-cutting study only. So, on the one hand, it enables to compare the width effect for residual stress distribution due to the flame-cutting and on the other hand, it allows evaluating the welding effect on a flame-cut plate. Regarding the temperature measurements for

the flame-cutting, they were performed on the cut axis 1 and 2. More details about its measurements are exposed in paragraph 3.2.3.

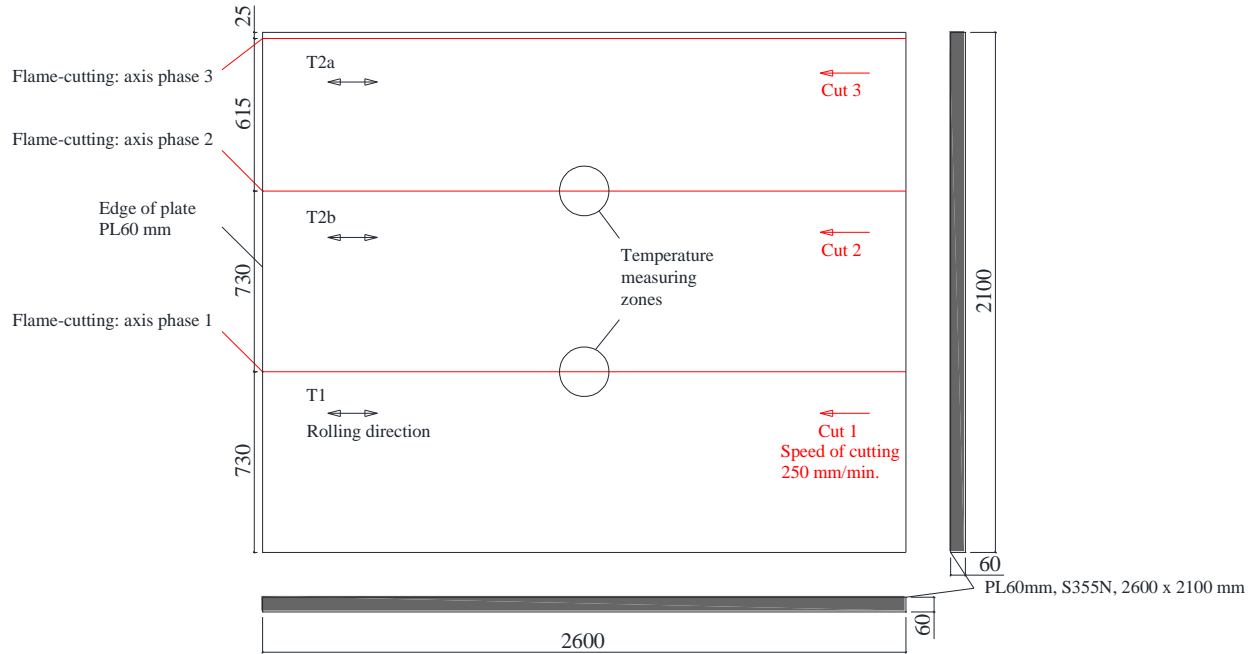


Figure 4: Plan view of flanges production and sequencing of the cuts (dimension in mm).

3.2.2 Welding

The type of welding used between T2b flange and the web is the submerged arc welding (SAW). This automatic or semi-automatic process is widely used in bridges construction for the advantages of: deep weld penetration, high speed welding, less distortion, good quality and control of the weld, etc. The principle of this method is based on an electrode continuously fed by a wire, and a flux constituted of granular particles of lime, silica and other compounds. The arc is formed under the flux (submerged arc) which a part is molted to form slag. The rest of flux is aspirated by the system and reused.

Regarding the experiment, the geometry of the weld is a tee-joint with 10 mm deposit metal. The fillets are composed of three passes accomplished simultaneously on each side of the web (Fig. 5).

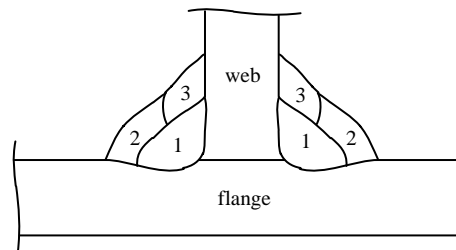


Figure 5: Distribution of welding passes.

The sequence follows a logical order; the first pass is welded on the corner between the web and the flange; the second pass is juxtaposed to the first one in order to support the third one. In the

plan, the web is welded parallel to long side of the flange (Fig. 6). In section, the web is centered with the flange. The welding was performed in the same direction as the rolling with an average speed of 6.66 mm/s. This process and the semi-automatic machine settings follow the welding procedure qualification record of the manufacturer.

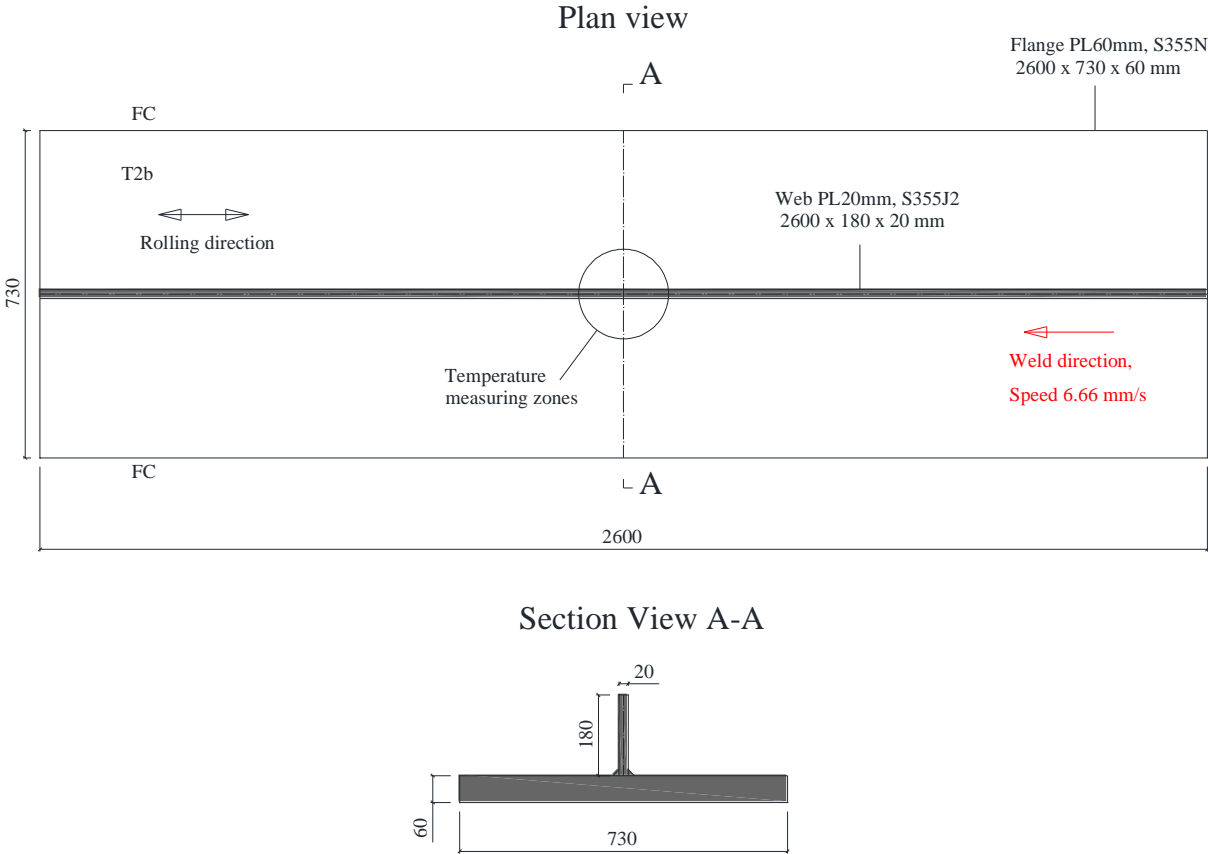


Figure 6: Plan and cut views of the welding process (dimension in mm).

As for the flame-cutting, temperature measurements were carried out in the middle of the plate and along the welding axis. More details are given in the following section.

3.2.3 Temperature measurements

The aim of these measurements is to obtain temperature curves as a function of the time for different locations of the plates. Thereafter, the data will be used to calibrate and compare the numerical models of flame-cutting and welding.

The measurements are taken by attaching thermocouples to the steel plates. Each thermocouple sensor is connected to a computer through an acquisition system. Fig. 7 presents the design of temperature measurements, including the locations of the thermocouple sensors.

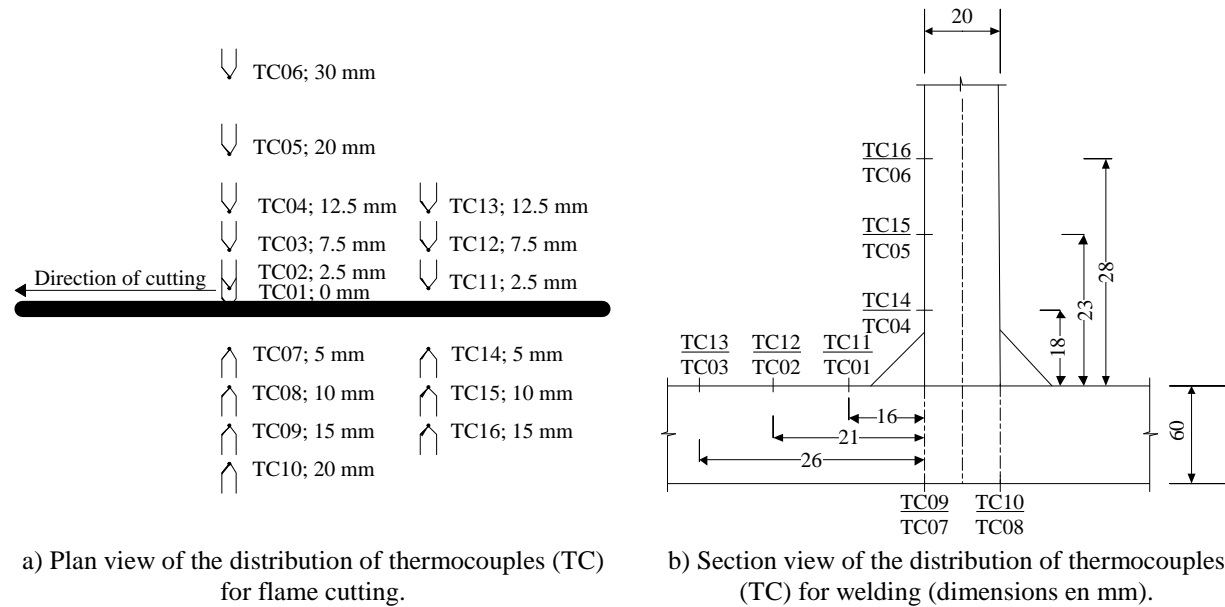


Figure 7: Design of temperature measurements.

As shown in Fig. 7, the design of the flame-cutting temperature measurement was planned to insure the repeatability of the data. Therefore, the sixty-four thermocouples are distributed over two sequences of cutting (cut 1 and 2), on two sections (Fig. 7a) and on both faces (upper and lower) of the plate. The first section is located at 1300 mm from the edge and consists of six sensors which are divided on both sides of the cut. Similarly, the second section consists of ten thermocouples situated 100 mm away from the first sensor section. These sensors were attached as close as possible to the cut in order to measure the higher temperatures.

Regarding the welding process (Fig. 6 and 7b) sixteen thermocouples were equally divided on the same cross sections as previously. Each section consists of two sensors located on the lower flange face, three on the upper flange face, and three on the web face. The main results of these measurements are presented in section 4.2.

3.3 Preparation of the specimens

3.3.1 Location of specimen

Each plate creates three specimens, see Fig. 8. Since the residual stresses represent internal stresses developed within a non-loaded element, they form a self-equilibrating system where the resultant force and moment are null. As a consequence these stresses are zero at the ends of the plate; and by Saint-Venant's principle, they must be maximum at a distance equal to the larger

transversal dimension of the piece. For this reason the specimen are located in the center of plate with a distance of 1.1 to 1.3 times the width plate.

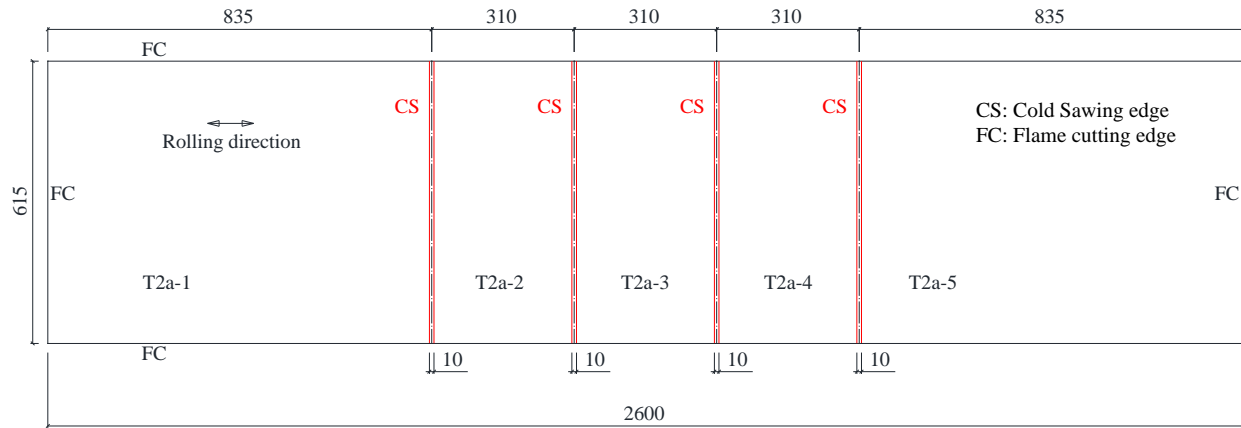


Figure 8: Location of the specimens (dimension in mm).

Of the nine total samples, six are devoted to the study of flame-cutting residual stresses (see Table 2). Furthermore, the influence of size is studied by comparing the results of 730 mm and 615 mm width. The other three specimens are dedicated to the study of flame-cutting and welding residual stresses.

Table 2: Table of specimens

Name	Origin of the residual stress FC : Flame cutting; W : Welding	Width (mm)	State S : Studied; IP : In progress
T1-2	FC	730	S
T1-3	FC	730	IP
T1-4	FC	730	IP
T2a-2	FC	615	IP
T2a-3	FC	615	S
T2a-4	FC	615	S
T2b-2	FC + W	730	IP
T2b-3	FC + W	730	IP
T2b-4	FC + W	730	IP

3.3.2 Design of sectioning and holes preparation

The number of strips depends on the distribution of the residual stresses. More precisely, in the locations where there is a strong gradient in residual stresses the strips must be thinner. Therefore, in order to obtain satisfying results, the strip width is thinner (10 mm) close to the flame-cut edges and welding zones, while it is thicker (20 mm) for the others zones, Fig. 9a, b and c.

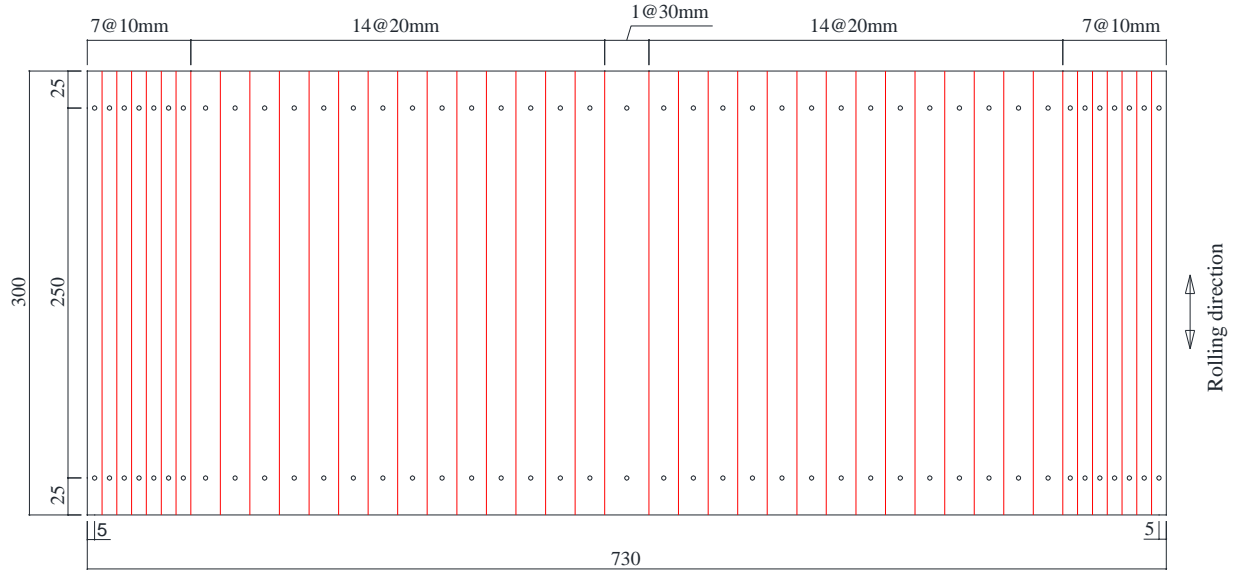


Figure 9a: Design of sectioning and holes measurements for flame-cut plates (view plan in mm).

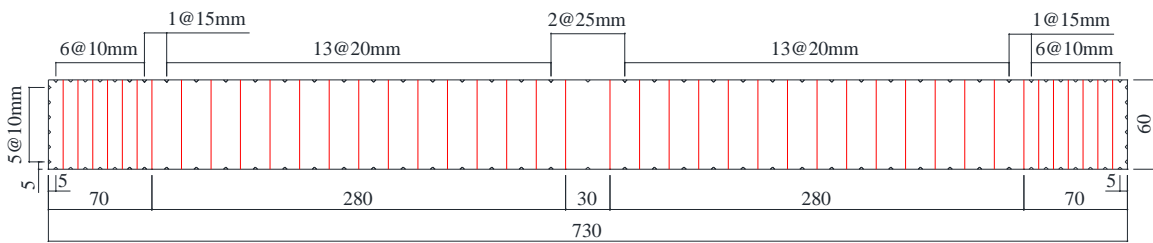


Figure 9b: Design of sectioning and holes measurements for flame-cut plates (section view in mm).

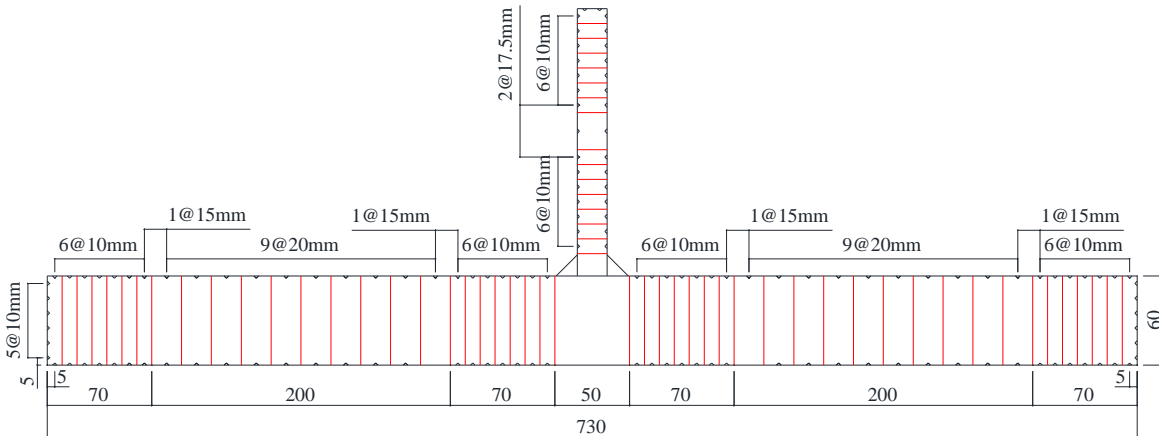


Figure 9c: Design of sectioning and holes measurements for flame-cut and welded plates (section view in mm).

Preparing the holes in each specimen requires care because the precision of the measurements depend directly on the quality of this step. Geometrically, each hole is located in the center of the strips with a constant distance of 250 mm. The size of the mark is adapted to the ball of the measuring instruments (see Fig. 10). In this experiment, creation of the hole requires four main steps. First, as precisely as possible, the location of the hole on the steel plates is determined by tracing. Second, preliminary marks are created using a punch bar with a basis measurement of

250 mm. Third, the holes are formed with the help of a center punch hit by a hammer. Finally, measurements are performed on each hole to verify the hole formation. As appropriate, some holes were corrected.

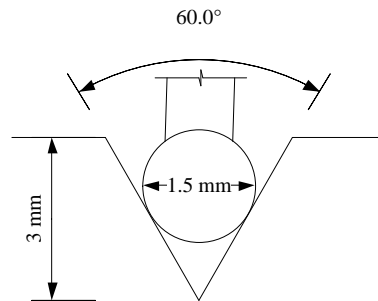


Figure 10: Detail of a hole measurement.

3.4 Procedure of measurements

The longitudinal measurements were performed by using a Huggenberger deformeter EDU250/10 adjusted on a 250mm measuring base (Huggenberger AG, 2012). The measurements were performed using steps cited in (Tebedge et al., 1973, Campana and Rupf, 2011) which are as follows:

- clean the holes with a compressed jet of air before taking any measurements;
- initialize the deformeter on the 250 mm bar invar before each measuring session;
- measure at least three time each distance to obtain a repeatability of the data;
- measure the bar invar before each series of measurements and after each ten readings;
- protect the holes from damage by covering with tape during the phase of moving, handling and sawing;

Much attention must be given to taking the initial measurements because, once the steel is cut, they cannot be repeated.

Regarding the data acquisition, the deformeter was directly connected to a laptop via a cable. This system allowed ten readings per second for each distance and saved the average value and the standard deviation. However, the reading is refused by the system if this deviation is more than 0.002 mm, and the distance has to be taken again.

3.5 Accuracy of measurement

Residual stress measurements are affected by various sources of errors. As the experiment takes place during several weeks and months, ambient temperature changes influence the material dilatation. In order to avoid this problem, as much as possible, measurement sessions were carried out in tent with a constant ambient temperature of 23°C. However few temperatures variations (less than 1°C) were measured. This error was measured by using a reference bar of the same material as the specimen but released of residual stress. This bar was put on the test pieces to follow the same temperature fluctuation and measure before each series of readings. Finally, it was noticed that the temperature error was smaller than the deformeter error. By consequence, this effect was neglected as it was not possible to measure it with enough accuracy.

The instrumental error due to the deformeter can be corrected by using a bar invar of 250 mm which constitute a fixed base. It is important to calibrate the device on this bar before each series

of measurements. However, even with this calibration, the precision error of the deformer provided by the supplier is +/- 0.005 mm on each average length (Huggenberger AG, 2012). The experimental error in term of stress is +/- 6 MPa.

Strips located at the edge were subjected to high stress gradients and were visibly curved after cutting. Consequently, the displacement measured by the deformer is the change in the chord length rather than the change in arc length which represents the actual strain. As mentioned, (Tebedge et al., 1973) the curvature effect can be assessed by measuring the offset δ and the change in chord length of the curved specimens. However, if the ratio of offset to length (δ/L) is lower than 0.001, the curvature correction has no significant influence on the strain calculation. As the curvature effect on the strain is smaller than the experimental error of the method of measurement in this study, the curvature correction was neglected.

4. Results and discussion

4.1 Calculation of residual stresses

Cutting allows an elongation of the compressed slices and an elongation and shortening of the slices in tension. Deformations measured before and after cutting are converted into stresses by assuming that the relaxation is purely linear elastic. The average length measured for each slice \bar{L} is defined by:

$$\bar{L} = \frac{1}{n} \sum_{j=1}^n L_j \quad (1)$$

where n is the number of measurements for one length (usually three) and L_j is the measured value distance for each step. So \bar{L}_i represent the initial measured of the length (before cutting) and \bar{L}_f the final measured of the length (after cutting). Then the strain due to relaxation of residual strain is:

$$\varepsilon_r = \frac{\Delta L}{L_i} = \frac{\bar{L}_f - \bar{L}_i}{\bar{L}_i} \quad (2)$$

By application of Hooke's Law, the residual stresses at the measured surface are:

$$\sigma_r = E\varepsilon_r \quad (3)$$

where E is Young's modulus (taken in first approximation equal to $210'000 \text{ N/mm}^2$).

Upper and a lower residual stresses, measured from both specimen surfaces, are named σ_{rU} and σ_{rL} respectively. Using Bernoulli's Law on plane sections, the average longitudinal stress σ_{ra} can be calculated as:

$$\sigma_{ra} = \frac{\sigma_{rU} + \sigma_{rL}}{2} \quad (4)$$

4.2 Temperature measurements

Temperature results are presented in Fig. 11. For the flame-cutting, six thermocouples at different location are plotted. It appears that the temperature increases rapidly when the torch passes near the sensors section. The different responses are consistent in shape and vary as a function of the position. Similarly, the welding temperature curves are presented with three peaks which correspond to each welding pass. In the welding curves, there are some differences with the initial values due to the non-uniform preheating of the steel plate prior to welding.

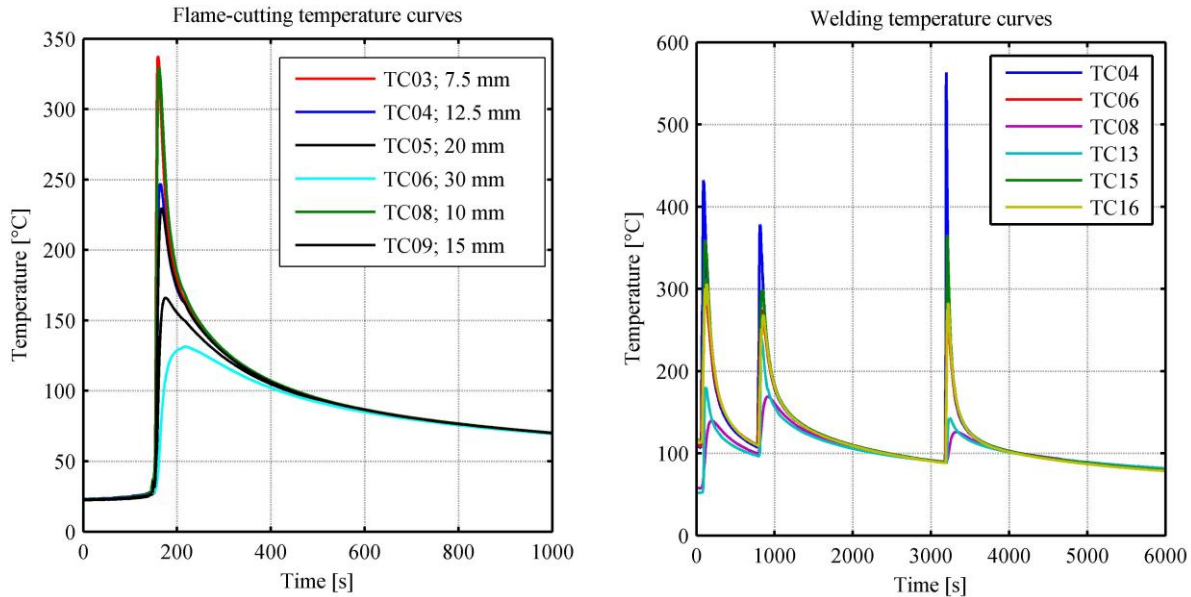


Figure 11: Temperature curves for flame-cutting and welding. For the locations of the thermocouples, see Fig. 7.

4.3 Flame Cutting

Fig. 12a, b and c show the residual stress distribution for each of the three flame-cut plates plotting the lower surface and the upper surface measurements, along with the average values. Fig. 12d summarizes the average residual stress values for all three plates. The three other specimens described in Table 2 are in progress of analyses.

The general shape of the distribution reveals that the curves have a high tensile residual stress at the flame cut edge which decreases rapidly with increasing distance from the edge. The tensile component is equilibrated to a certain extent by a compressive bloc near the edge (see Fig. 12).

The tension zone close to the edge in Fig. 12a, b, c show important stresses differences. It can be observed in general that upper side stress values are higher than the lower side stress values with a range up to 180 MPa. Due to the flame-cutting process the face hit by the torch is more heated than the other face. This observation is confirmed by the funnel shape of the heat affected zone (HAZ) in Fig. 13, where the heated zone is larger for the upper side. Residual stress study through the thickness would show the importance of this variation. Edges width tension can be assessed by linear interpolation in Fig. 12. The zone having high residual tensile stress is between 19 to 44 mm, which corresponds to 3-7 % of respective plate width. This range should be confirmed with further experiments results.

In Fig. 12d, the value of the average tensile residual stress varies between 231 MPa to 263 MPa, and the average maximum compressive residual stress varies between -55.0 MPa to -19.5 MPa. The maximum compressive stress occurs between 35 to 55 mm from the edge, which corresponds to 4-9 % of plate width. The tension zone and location of maximum compressive stress depends on several factors including: 1) the heat input created by the flame-cutting process, 2) the plate geometry and 3) the prior residual stresses due to rolling.

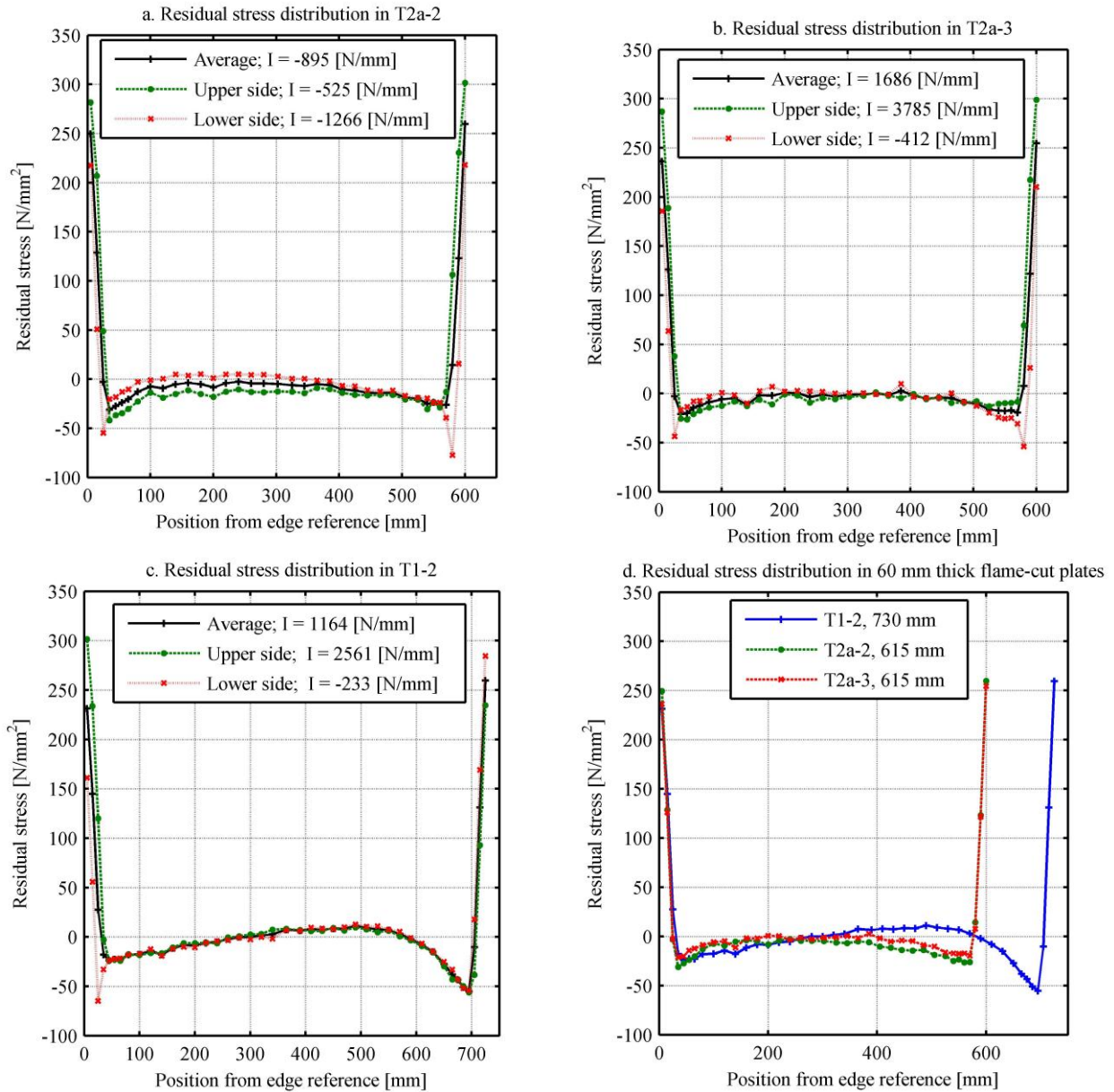


Figure 12: Results of residual stress distribution in 60 mm thick flame-cut plates.

The value “I” represented in Fig. 12a, b, c corresponds to the integration of the stresses over the section. Theoretically, due to self-equilibrium “I” should be zero. The first results of “I” show non-zero values which may be due to: 1) sawing, which modifies the residual stress state, 2) effect of residual stresses in the other directions and 3) accumulated experimental errors.

Residual stress at the center of the flame-cut plates varied between compression, tension, or zero. Over three plates (Fig. 12d), one shows only compression (T2a-2) with maximum value of -9.3 MPa, T2a-3 exposes a significant portion of practically zero residual stress and plate T1-2 exhibits even a tension zone with a maximum value of 11.1 MPa. The tension portion in the plate center indicates that the flame-cutting effect combined with the plate geometry is not higher than the prior tension residual stress due to rolling.

After three cut plates, it is difficult to show a real trend due to the width plate. However, in Fig. 12d the larger plate of 730 mm is characterized by a higher compressive residual stress at the edge and a higher tension residual stress at the center of the plate. These observations should be confirmed with more experiments.

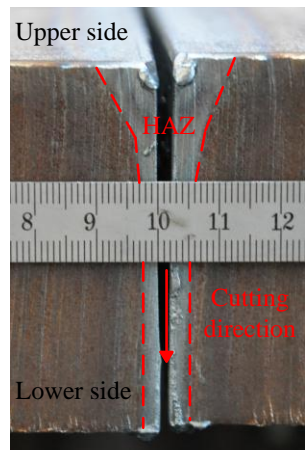


Figure 13: Section view of the flame-cutting heat affected zone (unit in mm).

5. Conclusions

Several methods exist to assess longitudinal residual stresses in steel; however, in the case of thick plates, the sectioning and the deep hole drilling methods are recommended. The sectioning method was selected in this study as the necessary equipment was available within the laboratory. If care is taken with the fabrication and preparation of the specimens, and a methodic and rigorous procedure of measurement is performed, the sectioning method can provide suitable and accurate results with an experimental error of ± 6 MPa.

Three plates over six flame cut specimens are analyzed in this study. Results of residual stress distribution show a high tensile residual stress at the flame cut edge equilibrated by a compressed zone. The maximum average value of the tensile residual stresses is 263 MPa whereas the maximum average value of compressive residual stress is -55.0 MPa. Residual stresses at the center of the flame-cut plates can be in compression, tension, or zero. Finally, main factors influencing flame-cut residual stress are: 1) the heat input 2) the plate geometry and 3) the prior residual stresses. Three other flame-cut specimens should be analyzed in order to consolidate the results. Furthermore, three flame-cut and welded plates must be investigated to determine the influence of welding on residual stress distribution.

Experimental results of residual stress measurements will serve to validate a numerical model which corresponds to flame-cut and welded plates used in bridge construction. The application of

this residual stress model will allow evaluation of resistance to lateral torsional buckling of steel bridge girders.

Acknowledgments

The authors would like to thank the material support of Zwahlen & Mayr (Aigle, Switzerland) for this research. In addition, the authors would like to thank Prof. Nicolas Boissonnade (College of Engineering and Architecture of Fribourg Switzerland) and Dr. Michel Thomann for their technical advice.

References

- ALPSTEN, G. A. & TALL, L. (1969). Residual stresses in heavy welded shapes. *In: RESEARCH, L. U. I. O. (ed.) Residual Stresses In Thick Welded Plates*. Fritz Laboratory Report 337.12.
- ASCENDORFF, K. K., BERNARD, A., BOERAEVE, P. & PLUMIER, A. (1983). "Le flambement de profilés européens de forte épaisseur." *Construction métallique*, 3.
- BJORHOVDE, R., BROZZETTI, J., ALPSTEN, G. & TALL, L. (1971). Residual Stresses in Thick Welded Plates. *In: RESEARCH, L. U. I. O. (ed.) Residual Stresses in Thick Welded Plates*. Fritz Engineering Laboratory report No. 337.13.
- BROZZETTI, J. (1969). Residual Stresses in Thick Plates. *In: RESEARCH, L. U. I. O. (ed.) Welding parameters and their effect on column strength*. Fritz Engineering Laboratory report No. 337.21.
- BRUNE, E. 2011. *Technique de soudage et de coupage*, Dagmersellen, PanGas Ag.
- CAMPANA, S. & RUPF, M. (2011). Procédure pour les mesures au défomètre. fisrt edition ed.: EPFL-ENAC-IIC-IBETON.
- CEN (2004a). EN 10 025-5. *Hot rolled products of structural steels - Part 5: Technical delivery conditions for structural steels with improved atmospheric corrosion resistance*. Brussels: European Committee for Standardization.
- CEN (2004b). EN 10025-1. *Hot rolled products of structural steels - Part 1: General technical delivery conditions*. Brussels: European Committee for Standardization.
- CEN (2004c). EN 10025-2. *Hot rolled products of structural steels - Part 2: Technical delivery conditions for non-alloy structural steels*. Brussels: European Committee for Standardization.
- CEN (2004d). EN 10025-3. *Hot rolled products of structural steels - Part 3: Technical delivery conditions for normalized/normalized rolled weldable fine grain structural steels*. Brussels: European Committee for Standardization.
- CEN (2004e). EN 10025-4. *Hot rolled products of structural steels - Part 4: Technical delivery conditions for thermomechanical rolled weldable fine grain structural steels*. Brussels: European Committee for Standardization.
- CEN (2005). EN 10027-1. *Designation systems for steels - Part 1: Steel names*. Brussels: European Committee for Standardization.
- DAVAINE, L. & LEBET, J. P. (2007). Lateral torsional buckling of steel-concrete composite bridge I-GIRDERS. *In: IABSE (ed.) Proceedings of the IABSE Symposium "Improving Infrastructure Worldwide"*.
- ECCS (1976). Manual on Stability of Steel Structures. Second Edition ed.
- ECCS (1984). Ultimate Limit State Calculation of Sway Frames with Rigid Joints. First Edition ed.
- GRIMAULT, J. P. & RONDAL, J. Etude comparative de différentes méthodes de mesure des contraintes résiduelles dans les profils creux en acier. *In: ACIER, C. D. C. E.-R. T. (ed.)*. Paris et Liège.
- HUGGENBERGER AG (2012). Deformeter DUII / EDUII.
- JOHANSSON, B., MAQUOI, R., SEDLACEK, G., MÜLLER, C. & BEG, D. (2007). Commentary and worked examples to EN 1993-1-5, Plated Structural Elements.
- LU, J. 1996. *Handbook of measurement of residual stresses*, Fairmont Press.
- LUGEON, M. & SRIRAMULU, V. (1978). Stabilité de poutres-colonnes métalliques en double té - Mesures des contraintes résiduelles (rapport d'essais).
- TEBEDGE, N., ALPSTEN, G. & TALL, L. (1973). "Residual-stress measurement by the sectioning method." *Experimental Mechanics*, 13, 88-96.
- WITHERS, P. J., TURSKI, M., EDWARDS, L., BOUCHARD, P. J. & BUTTLE, D. J. (2008). "Recent advances in residual stress measurement." *International Journal of Pressure Vessels and Piping*, 85, 118-127.